JOC Featured Article

pubs.acs.org/joc

Conformational Properties of the Germacradienolide 6-Epidesacetyllaurenobiolide by Theory and NMR Analyses

José E. Barquera-Lozada, Beatriz Quiroz-García, Leovigildo Quijano, and Gabriel Cuevas*

Instituto de Química, Universidad Nacional Autónoma de México, Circuito Exterior, Ciudad Universitaria, 04510 México D.F., Mexico

gecgb@servidor.unam.mx

Received October 8, 2009

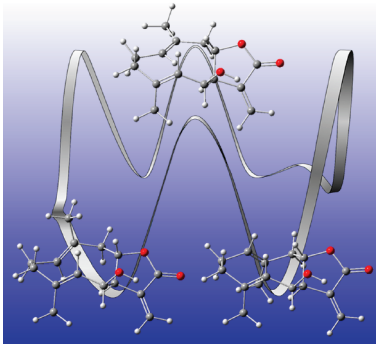

Knowing the conformational properties of 1(10),4-cyclodecadiene γ-lactones is important because of the biogenetic and evolutionary implications on the different groups of sesquiterpene lactones. Despite their importance, there are no physicochemical data on the conformational dynamic and the potential energy surface associated with the conformational changes of the cyclodecadiene ring. Fischer's biogenetic theory on the origin of ambrosanolides and helenanolides has support in the results presented since the conformers that yield two groups of sesquiterpene lactones coexist in solution as demonstrated by dynamic NMR experiments. These results are important on the basis of Fischer's proposal that states that the biosynthesis of each group of pseudoguaianolides requires a specific enzyme to select the right conformer to start the electrophilic cyclization. The germacra-1(10),4-dien-12,8α-olides can exist as a mixture of four different conformations, $[^{15}D_{5},{}_{1}D^{14}]$, $[{}_{15}D^{5},{}^{1}D_{14}]$, $[{}_{15}D^{5},{}_{1}D^{14}]$, and $[^{15}D_{5},{}^{1}D_{14}]$, and it is also proposed that the configuration of transannular cyclization depends on the conformation of the precursor. The results of the study presented herein show that 6-epi-desacetyllaurenobiolide exists in solution at room temperature as a mixture of two stable conformers, $[{}_{15}D^{5},{}^{1}D_{14}]$ and $[{}_{15}D^{5},{}_{1}D^{14}]$, which are more stable due to the diminishing of the so-called allylic strain. Analysis of the potential energy surface associated with the conformational interchange showed two other conformers that are intermediaries in the equilibria between $[{}_{15}D^{5},{}^{1}D_{14}]/[^{15}D_{5},{}^{1}D_{14}]$ and $[^{15}D_{5},{}_{1}D^{14}]/[{}_{15}D^{5},{}_{1}D^{14}]$. This indicates the presence of six different conformers participating in the global process instead of the four that have been proposed. The experimental values of $\Delta H^{\ddagger}$, $\Delta G^{\ddagger}$, ΔH_{conf}, and ΔG_{conf} of the conformational exchange and those calculated at the mPW1B95/6-31+G(d,p) level of theory are very similar, indicating that such level of theory is adequate for the description of this conformational equilibrium.

Introduction

Germacranolides are 1,5-cyclodecadienes that include two fragments of trisubstituted olefins located at interaction distance. In the case of epidesacetyllaurenobiolide (**1**, Figure 1), the two fragments are an alyllic alcohol (**2**) and a derivative of 2-butene (**3**). Germacranolides (**4**, Scheme 1) are characteristic metabolites of Asteraceae and are the precursors of guaianolides (**5**) and pseudoguaianolides (**6**) among other sesquiterpene lactones

DOI: 10.1021/jo902170w Published on Web 03/11/2010

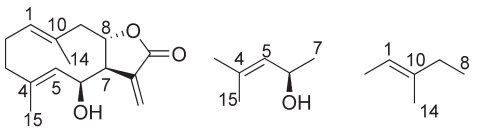

1 **2** **3**

FIGURE 1. Structures of 6-epidesacetyllaurenobiolide **1** and fragments **2** and **3** used to evaluate ring-independent interactions.

SCHEME 1. Intermediaries in the Biogenesis of Pseudoguaianolides (Germacranolide (4) → Guaianolide (5) → Pseudoguaianolide (6)) and the Origin of Ambrosanolides or Helenanolides by Cyclization Rearrangement of Two Conformers of an 4,5-Epoxygermacradienolide

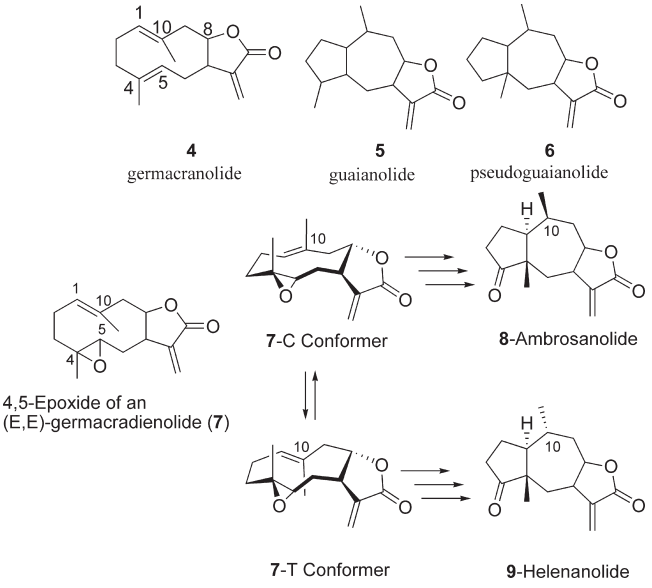

skeleta.[1−3] According to Fischer, the configuration of each of these natural products depends on the reacting conformation of the germacranolides during the cyclization.[1,4−13] For example, depending on which conformer of a 4,5-epoxygermacranolide (**7**, Scheme 1) an enzyme chooses, it produces pseudoguaianolides of the so-called

SCHEME 2. Conformational Equilibrium of Germacranolides

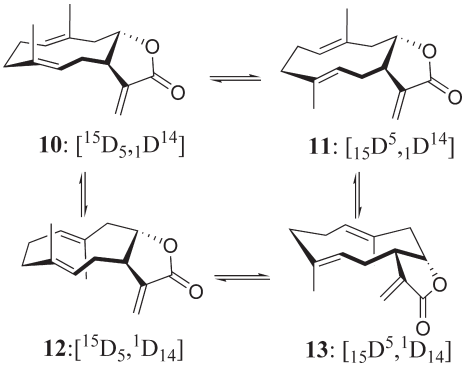

ambrosanolide type (**8**) or pseudoguaianolides of the helenanolide type (**9**). Both groups of compounds are epimeric isomers at C-10. Helenanolides have the *R* configuration with the methyl group at C-10 α-oriented, while in the epimeric ambrosanolides the methyl group at C-10 is *β*-oriented, corresponding to *S* configuration.[6] Generally, plants able to produce ambrosanolide-type sesquiterpenes are unable to produce helenanolide and viceversa.

Spectroscopic methods can be useful in studies of conformational mixtures and their rapid dynamic exchange.[14−20] The compounds containing 1,5-cyclodecadienes in their structures used in this study can exist as mixtures of several conformers that are very close in energy and are interchangeable through small energy barriers. Germacranolides, as well as cyclodecadienes, can have large conformational freedom. However, this freedom is restricted by the endocyclic double bonds and the *γ*-lactone ring fused to the cyclodecadiene that the germacranolides have. Four different main conformational forms have been proposed.[1,8,21] According to Samek's nomenclature,[22] these forms are described as the conformers [$^{15}D_5$,$_1D^{14}$] and [$_{15}D^5$,$^1D_{14}$] where double bonds C1−C10 and C4−C5 are cross oriented and the conformers [$_{15}D^5$,$_1D^{14}$] and [$^{15}D_5$,$^1D_{14}$] where the double bonds are parallel (Scheme 2). The four conformers are interchanged in a dynamic equilibrium through rotation of the bonds neighboring the C1−C10 and C4−C5 double bonds.

Several experimental[12,21,23−29] and theoretical (semiempirical models[8,12,24,25,30−33] and ab initio[34]) studies on conformational analysis of germacranolides have been

(1) Fischer, N. H. Sesquiterpene lactones: biogenesis and biomimetic transformations. *Recent Adv. Phytochem.* **1990**, *24*, 161–201.
(2) Cane, D. E. Sesquiterpene Biosynthesis: Cyclization Mechanisms. In *Comprehensive Natural Products Chemistry*; Cane, D. E., Ed.; Elsevier: New York, 1999; Vol. 2, pp 155−200.
(3) Fischer, N. H.; Olivier, E. J.; Fischer, H. D. *Fortschr. Chem. Org. Nat.* **1979**, *38*, 47–390.
(4) Takeda, K. *Tetrahedron* **1974**, *30*, 1525–34.
(5) Barquera-Lozada, J. E.; Cuevas, G. *J. Org. Chem.* **2009**, *74*, 874–883. Barquera-Lozada, J. E.; Cuevas, G. Computational simulation of terminal biogénesis of sesquiterpenes: the case of 8-epiconfertin. In *Quantum Biochemistry. Structure and Biological Activity*; Cherif, M., Ed.; Wiley-VCH: New York, 2009; pp 623−650.
(6) Fischer, N. H. *Rev. Latinoam. Quim.* **1978**, *9*, 41–6.
(7) Marco, J. A.; Sanzcervera, J. F.; Garcialliso, V.; Domingo, L. R.; Carda, M.; Rodriguez, S.; Lopezortiz, F.; Lex, J. *Liebigs Ann.* **1995**, 1837–1841.
(8) Tashkhodzhaev, B. T.; Abduazimov, B. K. *Khim. Prir. Soedin.* **1997**, 497–506.
(9) Messerotti, W.; Pagnoni, U. M.; Trave, R.; Zanasi, R.; Andreetti, G. D.; Bocelli, G.; Sgarabotto, P. *J. Chem. Soc., Perkin Trans. 2* **1978**, 217–24.
(10) Takeda, K. *Pure Appl. Chem.* **1970**, *21*, 181–203.
(11) El-Feraly, F.; Benigni, D. A.; McPhail, A. T. *J. Chem. Soc., Perkin Trans. 1* **1983**, 355–64.
(12) Shirahama, H.; Osawa, E.; Matsumoto, T. *J. Am. Chem. Soc.* **1980**, *102*, 3208–13.
(13) Takeda, K.; Horibe, I.; Minato, H. *J. Chem. Soc. C* **1970**, 1142–7.
(14) Brown, J.; Pawar, D. M.; Noe, E. A. *J. Org. Chem.* **2003**, *68*, 3420–3424.
(15) Ferreira, D. E. C.; De Almeida, W. B.; Dos Santos, H. F. *J. Theor. Comput. Chem.* **2007**, *6*, 281–299.
(16) Yavari, I.; Hosseini-Tabatabaei, M. R.; Nori-Shargh, D.; Jabbari, A. *THEOCHEM* **2001**, *574*, 9–17.
(17) Pawar, D. M.; Cain, D.; Gill, G.; Bain, A. D.; Sullivan, R. H.; Noe, E. A. *J. Org. Chem.* **2007**, *72*, 25–29.
(18) Pawar, D. M.; Miggins, S. D.; Smith, S. V.; Noe, E. A. *J. Org. Chem.* **1999**, *64*, 2418–2421.
(19) Pawar, D. M.; Noe, E. A. *J. Am. Chem. Soc.* **1996**, *118*, 12821–12825.
(20) Pawar, D. M.; Smith, S. V.; Mark, H. L.; Odom, R. M.; Noe, E. A. *J. Am. Chem. Soc.* **1998**, *120*, 10715–10720.
(21) Tori, K.; Horibe, I.; Tamura, Y.; Kuriyama, K.; Tada, H.; Takeda, K. *Tetrahedron Lett.* **1976**, 387–90.
(22) Samek, Z.; Harmatha, J. *Collect. Czech. Chem. Commun.* **1978**, *43*, 2779–99.
(23) Barrero, A. F.; Herrador, M. M.; Quilez, J. F.; Alvarez-Manzaneda, R.; Portal, D.; Gavin, J. A.; Gravalos, D. G.; Simmonds, M. S. J.; Blaney, W. M. *Phytochemistry* **1999**, *51*, 529–541.
(24) Faraldos, J. A.; Wu, S.; Chappell, J.; Coates, R. M. *Tetrahedron* **2007**, *63*, 7733–7742.

published, but none describe in detail the potential energy surface associated with the conformational equilibrium. Comprehending this equilibrium is critical to understand the biological reactivity of cyclodecadienes.

In a previous paper, we published the structure of the sesquiterpene lactone 6-epidesacetyllaurenobiolide (**1**, Figure 1), a 6-hydroxygermacra-1(10),4-dien-12,8α-olide isolated from *Montanoa grandiflora*.[35] The structure of this molecule was confirmed by single-crystal X-ray diffraction. The X-ray data demonstrated that the 10-membered ring exists in the crystal in a highly unusual boat−boat [$_{15}D^{5},_{1}D^{14}$] conformation (**11**) where the methyl group at C-4 is α-oriented and the methyl group at C-10 is β-oriented. This is in contrast with the common conformation [$^{15}D_{5},_{1}D^{14}$] (**10**, Scheme 2) of the costunolide-type structure (germacra-1(10),4-dien-12,6α-olides) where both methyl groups are above the plane of the 10-membered ring (β-oriented). It is known that sesquiterpene lactones of the costunolide-type are quite rigid structures, while germacra-1(10),4-dien-12,8α-olides are flexible.

In order to determine the conformational behavior of this kind of cyclodecadiene, we studied the 6-epidesacetyllaurenobiolide (**1**) in solution. The high-resolution ^{1}H NMR spectrum showed broadened signals while the ^{13}C NMR spectrum displayed 28 signals, almost double that expected for a sesquiterpene lactone. These facts suggest that compound **1** must exist at room temperature in solution as a conformational mixture in a dynamic equilibrium.

Methods

All the quantum chemical calculations were performed with Gaussian 03.[36] Geometries were optimized without geometry constraints using the density functional theory (DFT) hybrid method with mPWB95 functional.[37] Recent studies in small systems and in systems such as the molecules studied here have shown that the third-generation mPW1B95 functional produces more reliable thermochemical kinetic data than the B3LYP functional.[38,39] The double split valence polarized and diffuse 6-31+G(d,p) basis set was used for geometry optimization and frequency calculations. We used 6-31+G(d,p) basis functions due to the fact that addition of diffuse functions to double split valence basis has shown to be more important than increasing to a triplet split valence basis when calculating reaction energies and activation energies with DFT.[40] Finally, natural bond orbital (NBO) analysis was carried out with version 3.1 included in Gaussian 03.[41]

Theoretical NMR chemical shielding data were calculated at the VSXC/6-311+G(2d,2p) level with geometry calculated at the mPW1B95/6-31+G(d,p) level. The VSXC functional has better performance for calculating chemical shielding than other functionals, as recent studies have proved.[42] The spin−spin coupling constants were calculated with the B3LYP/cc-pVTZ method, which predicted with good accuracy J(HH) couplings.[43,44]

Compound **1** was obtained from *M. grandiflora* as is described in ref 35.

^{1}H and ^{13}C NMR spectra were measured at 500 and 125 MHz, respectively, in $CDCl_3$, toluene-d_8, and CD_3CN solutions, using TMS as internal standard. All signals were assigned on the basis of 1D and 2D NMR experimental data (DEPT, COSY, HSQC, and HMBC).

Thermochemical parameters ΔG, ΔH, $\Delta G^{\ddagger}$, and $\Delta H^{\ddagger}$ of conformational equilibriums were determined from variable-temperature ^{1}H NMR experiments measured in toluene-d_8. ΔG and ΔH were calculated by direct integration of the NMR signals at different temperatures, $\Delta G^{\ddagger}$ and $\Delta H^{\ddagger}$ were determined by line shape analysis using the gNMR program[45] in the coalescence proximity, where the experimental error in the determination of k is small.

Results and Discussion

The ^{1}H NMR spectrum of compound **1** at 500 MHz and room temperature showed broadened signals, while the ^{13}C spectrum showed 28 signals instead of the 15 signals expected for a sesquiterpene. This suggests a conformational equilibrium in solution. In order to find out which conformers take place in the conformational equilibrium, a computational study at the mPW1B95/6-31+G(d,p) level of theory was carried out. The results indicated that conformer [$_{15}D^{5},_{1}D^{14}$](**14**), the one with C15 α-oriented and C14 β-oriented (Figure 2), is more stable. This is the conformer observed in the solid state.[35] Conformer **14** is almost isoenergetic with conformer [$_{15}D^{5},^{1}D_{14}$](**15**), which has both methyl groups (C-15 and C-14) α-oriented (Figure 2), since it is only 0.39 kcal/mol less stable than the conformer **13**. Conformers [$^{15}D_{5},^{1}D_{14}$](**16**) and [$^{15}D_{5},_{1}D^{14}$](**17**) (Figure 2) were found to be much higher in energy, 3.72 and 3.87 kcal/mol less stable than **14**, respectively.

Differences in energy among the four conformers are very likely due to the rotation of the neighboring bonds to the double bond C4−C5, since rotation of the C1−C10 neighboring bonds practically does not change the energy. This behavior is inconsistent with the possibility that the stabilization could be due to a transannular interaction. Thus, the stabilization should lead to interaction of the double bond with the neighboring groups directly attached to it, i.e., the named allylic strain ($A^{1,3}$).[46−48] In order to evaluate these

(25) Jimeno, M. L.; Apreda-Rojas, M. D.; Cano, F. H.; Rodriguez, B. *Magn. Reson. Chem.* **2004**, *42*, 474–483.
(26) Ugliengo, P.; Appendino, G.; Chiari, G.; Viterbo, D. *J. Mol. Struct.* **1990**, *222*, 437–52.
(27) Wong, H. F.; Brown, G. D. *Phytochemistry* **2002**, *59*, 529–536.
(28) Watson, W. H.; Kashyap, R. P. *J. Org. Chem.* **1986**, *51*, 2521–4.
(29) Appendino, G.; Valle, M. G.; Gariboldi, P. *J. Chem. Soc., Perkin Trans. 1* **1986**, 1363–72.
(30) Milosavljevic, S.; Juranic, I.; Aljancic, I.; Vajs, V.; Todorovic, N. *J. Serb. Chem. Soc.* **2003**, *68*, 281–289.
(31) Tashkhodzhaev, B.; Makhmudov, M. K. *Khim. Prir. Soedin.* **1997**, 379–382.
(32) Turdybekov, K. M.; Edilbaeva, T. T. *Russ. Chem. Bull.* **1996**, *45*, 2741–2744.
(33) Turdybekov, K. M.; Edilbaeva, T. T. *Russ. Chem. Bull.* **1997**, *46*, 254–257.
(34) Maggio, A. M.; Barone, G.; Bruno, M.; Duca, D.; Rosselli, S. *J. Phys. Org. Chem.* **2005**, *18*, 1116–1122.
(35) Quijano, L.; Calderon, J. S.; Federico Gomez, G.; Jesus Lopez, P.; Rios, T.; Fronczek, F. R. *Phytochemistry* **1984**, *23*, 1971–4.
(36) Frisch, M. J. T. et al. Gaussian, Inc.: Wallingford, CT, 2004. See the Supporting Information for the full reference.
(37) Zhao, Y.; Truhlar, D. G. *J. Phys. Chem. A* **2004**, *108*, 6908–6918.
(38) Zhao, Y.; Pu, J. Z.; Lynch, B. J.; Truhlar, D. G. *Phys. Chem. Chem. Phys.* **2004**, *6*, 673–676.
(39) Zhao, Y.; Truhlar, D. G. *J. Phys. Chem. A* **2005**, *109*, 5656–5667.
(40) Lynch, B. J.; Zhao, Y.; Truhlar, D. G. *J. Phys. Chem. A* **2003**, *107*, 1384–1388.
(41) Glendening, E. D.; Reed, A. E.; Carpenter, J. E.; Weinhold, F. NBO version 3.1.
(42) Zhao, Y.; Truhlar, D. G. *J. Phys. Chem. A* **2008**, *112*, 6794–6799.
(43) Bagno, A.; Rastrelli, F.; Saielli, G. *Chem.—Eur. J.* **2006**, *12*, 5514–5525.
(44) Suardiaz, R.; Perez, C.; Crespo-Otero, R.; de la Vega, J. M. G.; Fabian, J. S. *J. Chem. Theory Comput.* **2008**, *4*, 448–456.
(45) Budzelaar, P. H. M. *gNMR 6.0 ed.*; IvorySoft: Centennial, CO, 2006.
(46) Allinger, N. L.; Hirsch, J. A.; Miller, M. A.; Tyminski, I. J. *J. Am. Chem. Soc.* **1968**, *90*, 5773–5780.
(47) Anslyn, E. V.; Dougherty, D. A. *Modern Physical Organic Chemistry*; University Science Books: Sausalito, CA, 2006.
(48) Johnson, F. *Chem. Rev.* **1968**, *68*, 375–413.

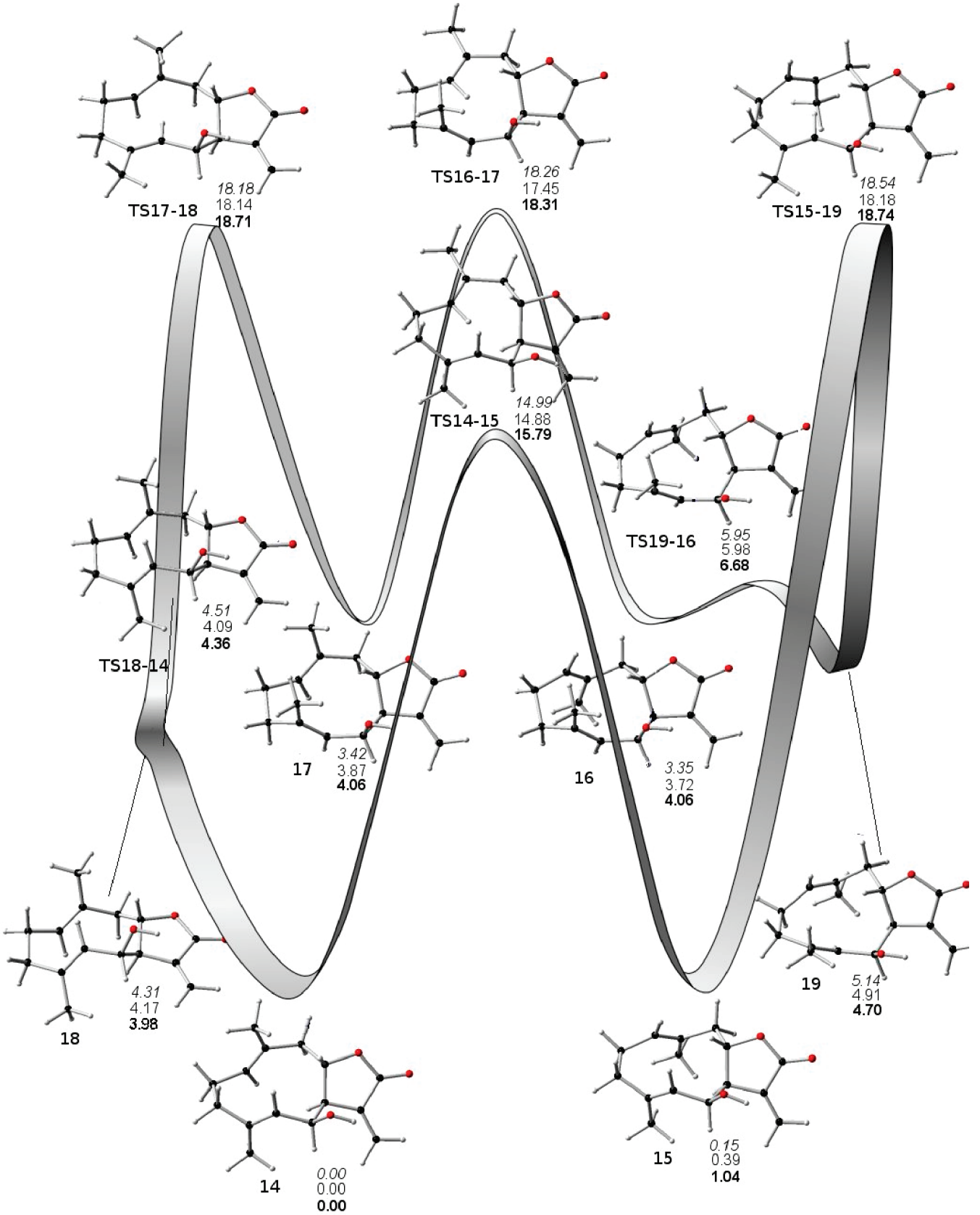

FIGURE 2. Conformers and conformational transition states in the potential energy surface of compound **1**. Relative energy (italic), zero point energy (ZPE) corrected relative energy, and relative free energy (bold) in kcal/mol.

interactions, the 4-methyl-3-penten-2-ol (**2**, Figure 1) was studied as a model of the C3−C4(C15)−C5C6−C7 segment of compound **1** but free of transannular interactions. Compound **2** was chosen as a good model for evaluating the

TABLE 1. Calculated Energies of Molecules 2 and 3 Used as Models of Two Fragments of Molecule 1[a]

model	frozen variables	dihedral (deg)	energies (kcal/mol)
2	C4−C5−C6−O	−159	0.00
		−168	0.22
		13	1.96
		17	1.95
	all		0.00
			0.04
			1.43
			1.57
3	all		0.00
			0.93
			2.08
			1.89

[a]The dihedral C4−C5−C6-O was frozen with dihedrals of conformers **14**−**17**. The energy of fragments **2** and **3** was also estimated by a single-point calculation with the geometry obtained from conformers **14**−**17**.

degree of contribution to the energy difference due to only the interaction between neighboring groups. To eliminate the strain due to the ring, the four conformers of **2** were optimized using the dihedral angle C4−C5−C6−O6 frozen at the geometries found for conformers **14**−**17**. The energy difference between conformers with the C6−H bond eclipsed with the double bond and conformers with the bond C6−O eclipsed is about 2 kcal/mol (Table 1). At the B3LYP/6-31+G(d,p) level, Cui et al.[49] found a similar value of 2.28 kcal/mol for the energy difference between both corresponding conformers in a similar system, pent-3-en-2-ol. The above findings indicate that the energy difference between conformers with C15 α-oriented (**14**, **15**) and those with C-15 β-oriented (**16**, **17**) in compound **1** is due to the $A^{1,3}$ strain. The rest of the energy difference between conformers **14**/**17** and **15**/**16** should be due to the other segment containing the double bond C10−C1 in the molecule (**3**, Figure 1). This assumption was supported by the calculated energies for those conformers in compound **3** with the corresponding frozen geometry of **14** and **15**, which showed higher stability compared with **17** and **16**, respectively. In this segment of the molecule, the energy difference should be only due to ring strain (vide supra), while the energy difference between **14**/**17** and **15**/**16** is due to ring strain and $A^{1,3}$ strain.

Small energy differences between **14**/**15** and **16**/**17** are due to rotation in the vicinity of the C10−C1 double bond, which has only one type of interaction, since it can be eclipsed only by C−H bonds. This fact suggested that the energy difference should come either from the ring strain or the transannular interaction. Molecule **3** allowed the estimation of the ring strain in the fragment C8−C9−C10(C14)−C1−C2 in molecule **1**. In this case, a single-point energy determination for the conformers of **3** with the geometry corresponding to **14**−**17** (Table 1) were calculated. The use of molecule **2** with all coordinates frozen made possible the estimation of ring strain plus $A^{1,3}$ strain.

The energy difference between **14** and **15** cannot be due only to the energy difference calculated from the model molecule **3** because the difference is quite large. The difference of the all frozen molecule **2**, is very small. Then, the energy difference could be also due to the transannular interaction of the double bonds. This is supported by the NBO analysis of the C4═C5 → C1═C10* interaction which was found to be 0.2 kcal/mol for **14**, while the same interaction for **15** was 0.89 kcal/mol. These values could account for the energy difference between **14** and **15** when molecule **3** is taken as a model. The interaction in the other direction C1═C10 → C4═C5* is too small to be considered (0.01 for kcal/mol for **14** and 0.09 kcal/mol for **15**). Although the reason for this difference is not clear, it could be related to an effect of the allylic substitution. For conformers **16** and **17**, the C4═C5 → C1═C10* interaction is 0.1 kcal/mol for **16** and 0.6 kcal/mol for **17**. Thus, the energy differences between **14**/**15** and **16**/**17** could be due to the balance of the ring strain and the transannular interaction.

The small energy difference between the conformers of lower energy indicates that they must coexist in solution. In order to confirm the above assumption, a variable-temperature ^{1}H NMR study at 500 MHz was carried out. At −20 °C in CD_3CN, duplicated signals were observed for almost all hydrogen atoms in the molecule indicating the existence of two different conformers (see the Supporting Information). For example, at higher frequencies, the typical pair of doublets due to the exocyclic methylene protons conjugated with the γ-lactone (H13a and H13b) were observed as two pairs of doublets at δ 5.83/5.85 (H-13a) and 6.28/6.30 (H13b). A triplet at δ 5.12 is assigned to H1 of the main conformer (**14**), while two overlapped doublets at δ 5.07 and 5.04 were assigned to H5 and H1 of the minor conformer (**15**), respectively (Figure 3, above). The broad doublet at δ 4.89 corresponds to H5 of the main conformer. Two overlapped signals at δ 4.71 and 4.72 are assigned to H6 and H8 of main and minor conformers, respectively, while well-resolved signals for H6 and H8 for the minor and main conformers appeared at δ 4.62 and 4.56, respectively.

The spectrum recorded at −20 °C in toluene-d_8 (see the Supporting Information), showed similar results, but in this case diamagnetic and paramagnetic shifts due to the aromatic character of the solvent promote better resolution of some other signals. Therefore, very well resolved signals for H5 belonging to the main and minor conformers were observed at δ 4.90 for the former and 5.01 for the latter (Figure 3, bottom). Thus, the integration of both signals gave the relative proportions of conformers **14**/**15** as 62:38.

In order to confirm which conformers were present in solution, besides the theoretical calculation of their energies, ^{13}C chemical shifts of the four conformers (**14**−**17**) were calculated at level VSXC/6-311+G(2d,2p) and compared with the experimental ones measured in CD_3CN at −20 °C. The smallest root mean squares (rms) of the differences between experimental and calculated chemical shifts correspond to the signals of the minor conformer **15** (Table 2). In the case of the signals corresponding to the main conformer, these are in good agreement with the calculated chemical shifts for conformer **14**. For example, C1, which is one of the carbon atoms directly involved in the conformational equilibrium, drastically changes its chemical environment in both conformers showing a difference between calculated and experimental values of 4.38 ppm for the main conformer **14** and 9.56 ppm for the minor one. Conversely, in the case of conformer **15**, the differences are 4.53 and 0.65 ppm, respectively.

The rms of chemical shift differences provide a good estimation of which signals belong to each conformer, but

(49) Cui, M.; Adam, W.; Shen, J. H.; Luo, X. M.; Tan, X. J.; Chen, K. X.; Ji, R. Y.; Jiang, H. L. *J. Org. Chem.* **2002**, *67*, 1427–1435.

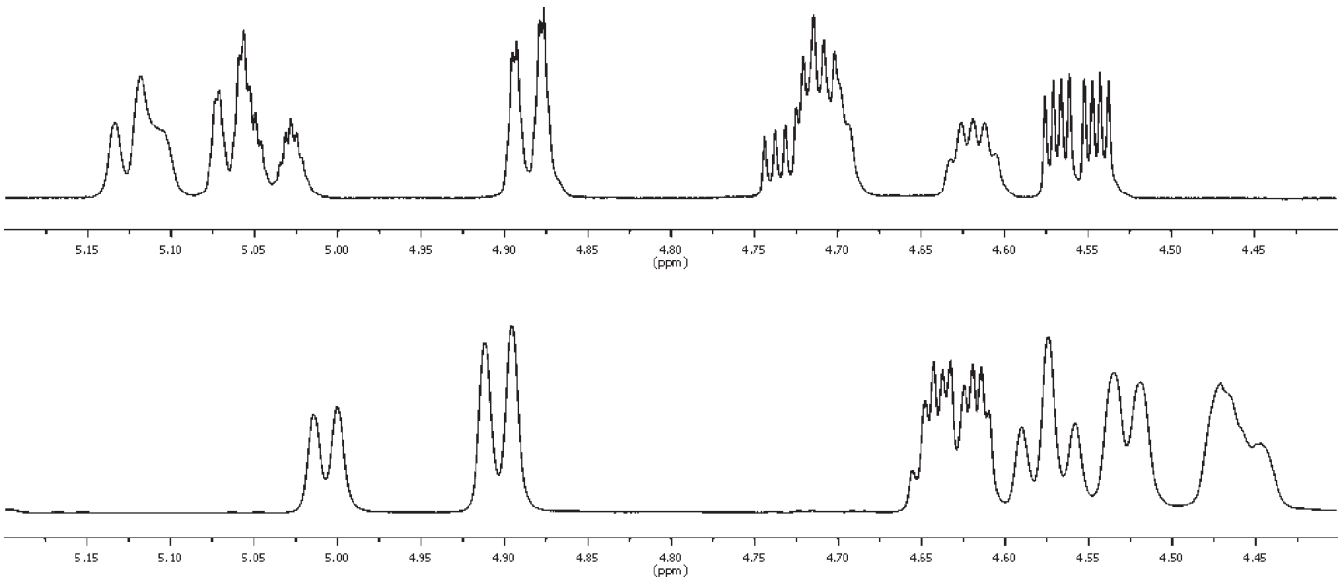

FIGURE 3. (Top) 500 MHz ^{1}H NMR spectrum region from 4.49 to 5.18 ppm of **1** in CD_3CN at −20 °C. (Bottom) 500 MHz ^{1}H NMR spectrum region from 4.39 to 5.8 ppm of **1** in toluene-d_8 at −20 °C.

TABLE 2. Differences between ^{13}C NMR Chemical Shifts of 1 Dissolved in CD_3CN at −20 °C and Chemical Shifts of 1 Calculated at the VSXC/6-311+G(2d,2p) Level

	main conformer				
	expt	**Δ14**	**Δ15**	**Δ16**	**Δ17**
C1	126.25	4.38	−4.53	1.00	−2.90
C2	24.63	−7.34	−6.14	−5.49	−5.82
C3	37.22	−8.29	−8.85	−10.29	−10.55
C4	135.76	−1.49	−2.91	−3.47	−4.03
C5	129.92	3.96	1.85	7.06	4.88
C6	70.02	−7.51	−10.00	−12.11	−11.42
C7	51.52	−7.81	−5.42	−9.30	−11.27
C8	76.91	−1.80	−4.99	−9.92	−4.16
C9	46.45	−8.09	−0.31	−3.26	−8.40
C10	133.32	−2.78	3.76	−0.99	1.29
C11	137.85	0.48	0.79	0.44	−0.28
C12	170.84	10.54	10.03	10.78	10.63
C13	123.38	6.41	5.52	6.80	7.20
C14	17.36	−3.07	−8.43	−7.11	−3.01
C15	16.42	−2.95	−3.92	−2.26	−2.26
	rms	**5.91**	5.97	7.12	6.93
	minor conformer				
	expt	**Δ14**	**Δ15**	**Δ16**	**Δ17**
C1	131.43	9.56	0.65	6.18	2.28
C2	25.04	−6.93	−5.73	−5.08	−5.41
C3	38.77	−6.74	−7.30	−8.74	−9.00
C4	135.99	−1.26	−2.68	−3.24	−3.80
C5	131.73	5.77	3.66	8.87	6.69
C6	70.89	−6.64	−9.13	−11.24	−10.55
C7	49.26	−10.07	−7.68	−11.56	−13.53
C8	79.31	0.60	−2.59	−7.52	−1.76
C9	40.90	−13.64	−5.86	−8.81	−13.95
C10					
C11	137.70	0.33	0.64	0.29	−0.43
C12					
C13	123.70	6.73	5.84	7.12	7.52
C14	21.18	0.75	−4.61	−3.29	0.81
C15	16.56	−2.81	−3.78	−2.12	−2.12
	rms	6.82	**5.27**	7.28	7.49

they are not conclusive because the difference between the rms is in some cases too small. For this reason, coupling constants ^3J(H5−H6), ^3J (H6−H7), ^3J (H7−H8), ^3J (H8−H9α), ^3J (H8−H9β), and ^3J (H9α-H9β), which are the ones directly involved in the conformational change, were also calculated at the B3LYP/cc-pVTZ level and compared with the experimental values (Table 3). In this case, the rms of the differences between calculated and experimental coupling constants clearly indicated that conformer **14** is the most stable, followed by conformer **15**.

TABLE 3. Differences between ^{1}H Couplings of 1 Dissolved in CD_3CN at −20 °C and Chemical Shifts of 1 Calculated at the B3LYP/cc-pVTZ Level

	main conformer				
coupling	expt	**Δ14**	**Δ15**	**Δ16**	**Δ17**
^3J(H5−H6)	7	−0.06	−1.57	−3.23	−2.28
^3J (H6−H7)	3	−0.3	0.3	−0.58	−1.17
^3J (H7−H8)	5	−1.04	−2.84	−1.06	−0.42
^3J (H8−H9β)	2.5	0.07	3.67	1.55	2.72
^3J (H8−H9α)	12	−1.67	−1.36	−1.74	−3.63
^3J (H9α-H9β)	12	−0.3	1.5	0.71	0.49
	rms	**0.822**	2.168	1.724	2.143
	minor conformer				
	expt	**Δ14**	**Δ15**	**Δ16**	**Δ17**
^3J(H5−H6)	7	−0.06	−1.57	−3.23	−2.28
^3J (H6−H7)	3	−0.3	0.3	−0.58	−1.17
^3J (H7−H8)	3	0.96	−0.84	0.94	1.58
^3J (H8−H9β)	6	−3.43	0.17	−1.95	−0.78
^3J (H8−H9α)	11.5	−1.17	−0.86	−1.24	−3.13
^3J (H9α-H9β)	13.5	−1.8	0	−0.79	−1.01
	rms	1.702	**0.819**	1.714	1.848

The potential energy surface gives a good idea of the interchange of conformers **14**−**17**. In all transition states (TS) generated by rotation of the C4−C5 and C1−C10 neighboring bonds, the hydrogen attached to the double bond is oriented inside the ring (Figure 2). The activation free energy for interchanging conformers **14** and **15** was found to be 15.79 kcal/mol (Table 4). This is a value large enough to allow the observation of the interchange between them with DNMR. Comparatively, the conformational barrier for cyclohexane is about 10 kcal/mol.[50]

(50) del Fernandez-Alonso Maria, C.; Canada, J.; Jimenez-Barbero, J.; Cuevas, G. *ChemPhysChem* **2005**, *6*, 671–80.

TABLE 4. Activation Energies (kcal/mol) at mPW1B95/6-31+G(d,p)

	E_{act}	$E_{act}+0$	$\Delta G^{\ddagger}$
TS14−15	14.99	14.88	15.79
TS15−19	18.39	17.79	17.70
TS19−16	0.81	1.06	1.98
TS16−17	14.90	14.02	14.24
TS17−18	14.76	14.28	14.64
TS18−14	0.20	−0.09	0.39

Between conformers **15** and **16**, an energy minimum corresponding to an intermediate conformer (**19**), similar to **16** with C14 α-oriented and C15 *β*-oriented, but with a dihedral angle H2*β*−C2−C3−H3*β* rotated clockwise by 80.8° (Figure 2) was observed. Conformer **19** is necessary for interchanging conformers **15** and **16**. Similarly, in the interchange between conformers **17** and **14**, a minimum corresponding to conformer **18** was found. Here, the rotation of the dihedral angle H2*β*−C2−C3−H3*β* is counterclockwise.

The energetic barrier for transformation of conformer **15** to **19** was found to be the highest (18.39 kcal/mol), with conformer **15** being more stable than **19** (ΔE = 4.99 kcal/mol). On other hand, the energetic barrier between conformers **19** and **16** is less than 1 kcal/mol. In addition, conformer **16** is 1.79 kcal/mol more stable than **19** indicating a fast equilibrium between them. The activation energies for the elemental steps in the conformational interchange **16**/**17** and **17**/**18** are very similar with values around 15 kcal/mol. In contrast, in the case of **18**/**14**, it is very small, so the correction by zero-point energy causes the barrier to disappear leading to a quick accumulation of **14** due to its higher stability when compared with **18**. Although the energetic barrier for dihedral H2*β*−C2−C3−H3*β* rotation is very small, this happens only when the C4−C5 double bond changes its orientation but there is no rotation when the C1−C10 double bond changes. This is because the C10−C5−H transannular angle value in conformer **14** is 73°, while in **18** it is 56°. Similarly, in the case of conformers **16** and **19**, these values are 74° and 53°, respectively. The instability of conformers **18** and **19** is due to the inside orientation of C5−H bond, which is closer to the plane of the ring compared with **14** and **16**; this orientation generates a steric repulsion between the H atom and the ring.

The ΔH, ΔG, $\Delta H^{\ddagger}$, and $\Delta G^{\ddagger}$ calculated values of the conformational equilibrium between the stationary states **14** and **15** at level mPW1B95/6-31+G(d,p) were compared with the experimental values obtained using the ^{1}H NMR spectral data measured in toluene-d_8. Integration of the well-resolved signals for both conformers, H5, allowed the determination of experimental values of the ΔH and ΔG associated with the conformational equilibrium (Table 5). Determination of ΔH was not possible because integration values of the signals do not show significant changes with temperature, so ΔH value must be close to cero.

Experimental values of $\Delta H^{\ddagger}$ and $\Delta G^{\ddagger}$ were obtained through the line shape analysis of the ^{1}H NMR spectra at different temperatures. Figure 4 shows the experimental and simulated spectra using the gNMR program[45] in the region of frequencies of H5 signals, at different temperatures. The experimental value of $\Delta G^{\ddagger}$ at 25 °C was determined directly from the rate constant (k) value obtained with gNMR program, while the experimental $\Delta H^{\ddagger}$ was determined by

TABLE 5. Experimental and Calculated Energies (kcal/mol) of Conformational Equilibrium between 14 and 15

	mPW1B95	expt
ΔG	1.04	0.32
$\Delta G^{\ddagger}$	15.79	15.71
$\Delta H^{\ddagger}$	14.43	14.66

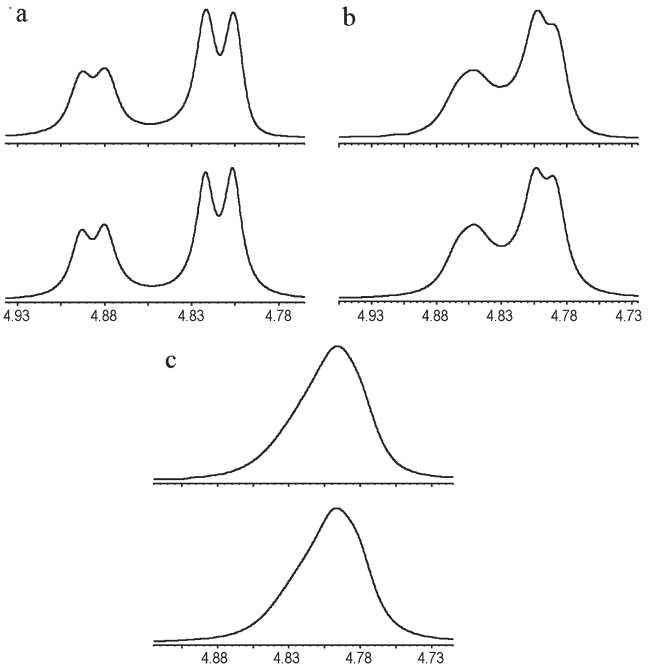

FIGURE 4. Experimental (top) and simulated (bottom) spectra of compound **1** at (a) 12 °C, (b) 24 °C, and (c) 36 °C.

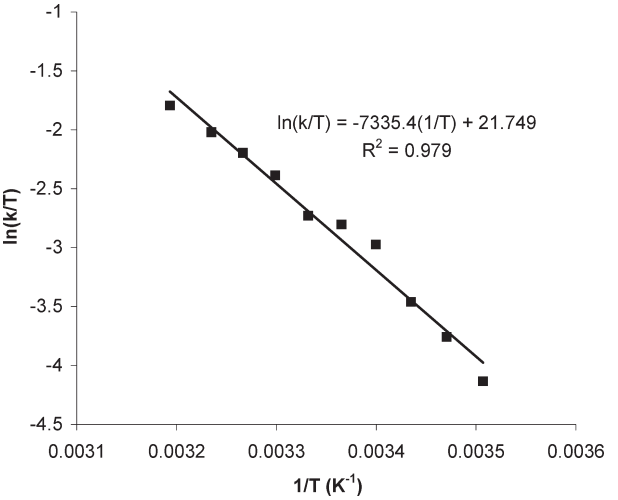

FIGURE 5. Linear regression for experimental k at different T.

adjusting the k values obtained at different temperatures using eq 1 (Figure 5):

$$\ln\frac{k}{T} = -\frac{\Delta H^{\ddagger}}{R}\left(\frac{1}{T}\right) + \frac{\Delta S^{\ddagger}}{R} + \ln\left(\frac{k_B}{h}\right) \qquad (1)$$

The calculated and experimental data are in good agreement and give a good prediction of the stability order indicating that the level of theory was adequate. The differences between the experimental and calculated $\Delta H^{\ddagger}$ and $\Delta G^{\ddagger}$ are also very small. In the case of ΔG, the difference is more significant, but this is expected because the ΔG value associated with the conformational equilibrium is small. Nevertheless, the differences between calculated and experimental values are less than 1 kcal/mol.

Conclusions

In solution, 6-epidesacetyllaurenobiolide (**1**) exists as a mixture of conformers **14** and **15**. In both conformers, the methyl group at C4 (C15) is α-oriented. The conformers with C15 β-oriented are by far less stable mainly due to the allylic strain generated when C15 is eclipsed by the oxygen atom of the hydroxyl group at C6. The small energy differences between **14** and **15** are due to a balance of effects: first, the transannular interactions favoring conformer **15**, and second, the ring strain generated in the segment **3** that favors conformer **14**. For the interchange between conformers **14** and **15** ΔG is 0.32 kcal/mol with a barrier of 15.71 kcal/mol.

In the potential energy surface of **1** we found two extra conformers (**18** and **19**) that, as far as we know, have not been described previously. Although **18** and **19** are not energetically favored, they are intermediates in the conformational equilibrium between **15** and **16** and between **17** and **4**, respectively.

The results presented herein fully support Fischer's biogenetical proposal since the major conformers **14** and **15** are expected to be quite similar to those of the key 4, 5-epoxygermacradienolide intermediates (Scheme 1) with respect to structures and energies, giving place to ambrosanolides and helenanolides. Plants producing them require enzymes capable of selecting the right conformer for the electrophilic cyclization. Nevertheless, our results do not actually rule out the alternative biogenesis proceeding through an (*E*/*Z*)-germacradienolide and its 4, 5-epoxide.

Acknowledgment. J.E.B.-L. acknowledges Conacyt for financial support. This work was financially supported by Consejo Nacional de Ciencia y Tecnología (CONACYT) via Grant No. 49921-Q and by DGAPA Grant No. IN-203510-3. We are also grateful to DGSCA, UNAM for supercomputer time. We are also grateful to Rebeca López-García for the revision of the English version of this manuscript and to the reviewers for their useful comments that led to the improvement of this article.

Supporting Information Available: Full optimized geometries of all compounds, NMR spectra, and full ref 36. This material is available free of charge via the Internet at http://pubs.acs.org.